From clusters to the solid state: Global minimum structures for cesium clusters Cs_n $(n=2-20,\infty)$ and their electronic properties

Behnam Assadollahzadeh, Christian Thierfelder, and Peter Schwerdtfeger*
Centre for Theoretical Chemistry and Physics, The New Zealand Institute for Advanced Study, Massey University (Auckland Campus), Private Bag 102904, North Shore MSC, 0745 Auckland, New Zealand

(Received 25 August 2008; revised manuscript received 23 November 2008; published 24 December 2008)

A systematic search for the global minimum structures of neutral cesium clusters with up to 20 atoms is performed utilizing a density-based genetic algorithm within density-functional theory in a scalar-relativistic pseudopotential formalism. The transition from two- to three-dimensional structures is found to be ambiguous and no unique growth pattern could be identified. Previously proposed icosahedral structure growth could not be verified within this size regime. Using a calibrated static dipole polarizability for atomic cesium to density functionals, the evolution of this property with increasing cluster size is discussed and compared to other alkali-metal clusters. For each cluster size, electronic properties are calculated and compared to available experimental data, and the extrapolation to the bulk limit is discussed.

DOI: 10.1103/PhysRevB.78.245423 PACS number(s): 36.40.Cg, 73.22.−f, 71.15.Nc

I. INTRODUCTION

Clusters of the first main group elements represent the simplest metal clusters to be studied theoretically due to their basic electronic structure involving only valence *s* electrons with a core that is only slightly polarized. They have therefore been used as an ante-type system for understanding size dependencies of electronic effects in metal clusters. Indeed, the synthesis of sodium clusters by Knight *et al.*[1] and de Heer,[2] the detection of an electronic shell structure, the measurement of their static electric-dipole polarizabilities,[3] and their interpretation in terms of the jellium model[4,5] can all be regarded as one of the causes that generated extensive research in metal cluster physics. Alkali-metal clusters are among the most polarizable elements,[6] and Knight *et al.*,[1] who pioneered the experimental work on sodium clusters, revealed that polarizabilities slowly decrease towards the bulk limit as the cluster size increases.

Cesium enjoys a rather exceptional position within the group 1 elements. It has the largest polarizability and smallest ionization potential as relativistic corrections (decrease in the polarizability by 16% and increase in the ionization potential by 3.8%[7]) are not quite large enough to reverse the trend down the Periodic Table.[8] This happens at francium, in contrast to the group 11 elements where already at gold relativistic effects are so large to reverse major trends in electronic properties.[9,10] In comparison, electron correlation from the 5*sp* core decreases the polarizability by 4%.[11] This unique position is also confirmed by substantial experimental and theoretical studies on the polarizabilities and structural properties of homonuclear and heteronuclear lithium,[12–24] sodium,[1,3,6,13,15,20,25–35] potassium clusters,[20,36–39] and rubidium clusters[40–42] to quote some. To our knowledge there is, however, only one theoretical study on polarizabilities of small neutral cesium clusters, and experimental measurements for this property are not available. Moreover, experimental or theoretical data on structural and physical properties of small cesium clusters are very scarce.[43–45]

Regarding the atomic polarizability of cesium, Hall and Zorn[46] deflected a velocity-selected cluster beam via an inhomogeneous electric field and probed (63.3 ± 4.6) Å^3, Molof *et al.*,[47] who utilized the *E-H*-gradient balance technique, obtained (59.6 ± 1.2) Å^3, and most recently, Amini and Gould[11] measured (59.43 ± 0.08) Å^3 also via beam deflection. Lim *et al.*[48] applied the Douglas-Kroll-Hess coupled-cluster with single and double substitutions including perturbative triples [CCSD(T)] method and report a polarizability of 58.69 Å^3. Derevianko *et al.*[49] calculated 59.49 Å^3 by utilizing a relativistic single-double all-order method and report discrepancies to experimental results for atomic polarizabilities of sodium, potassium, rubidium, and cesium of less than 2%. It is also noteworthy to mention a few measurements and calculations of Stark shifts and lifetimes, which are reported in Refs. 50–55, spectroscopic data for dimeric cesium,[56–59] photoabsorption spectra,[60–63] and photodetachment spectra for small cesium clusters.[64–66] The electron affinity of atomic cesium is also discussed in a review of Andersen *et al.*[67]

Regarding cluster studies, Gspann[68] synthesized large cesium clusters with up to 2500 atoms per cluster from pure vapor expansion and investigated their velocity distributions. Martin and co-workers[69] observed electronic shell structures in heteronuclear Cs-O clusters. Krauss and Stevens[45] calculated the polarizabilities of cesium cluster chains with four and six atoms, respectively, and also employed a rhomboidal (Cs_4) and a planar triangular (Cs_6) geometry. They utilized pseudopotentials at the Hartree-Fock (HF), configuration interaction (CI), and Moller-Plesset (MP2/MP4) levels of theory and found the chainlike structures to exhibit markedly higher polarizabilities as expected. Geometric and electronic structures of neutral Cs_n and Cs_nO clusters, up to $n=70$, obtained by means of a density-functional-theory (DFT)-based spherical average pseudopotential method are discussed by Borstel and co-workers.[70,71] Using a many-body potential based on local-density calculations, Blaisten–Barojas and co-workers[72] calculated the geometry of neutral Na, K, Rb, and Cs clusters with up to 310 atoms. Their potentials were satisfactory in describing the structural properties of the respective bulk metals. Furthermore, they studied the dynamics of fission mechanisms and summarized that

the cluster size at which multiply charged clusters undergo fission strongly depends on the temperature. In a similar fashion, Lai *et al.*[73] used a Gupta-type many-body potential to account for the interactions between alkali-metal clusters and employed a genetic algorithm and a basin hopping method to locate the global energy minima of clusters with up to 56 atoms. They report identical global minimum structures for the alkali-metal clusters independent of the search algorithm and describe the growth pattern of neutral Na, K, Rb, and Cs clusters as icosahedral-like. It should be mentioned that they find overall, with only few exceptions, identical global minimum structures for all four monovalent metal clusters. However, the Gupta potential does not perform well for the energetics of small clusters, as it does not describe many-body effects correctly.[74] Employing all-electron CI, MP2, and DFT levels of theory, Maity and co-workers[75] studied the geometric and electronic properties of neutral and singly positively charged cesium clusters with up to ten atoms. They conclude that Cs_7 adopts a three-dimensional (3D) structure whereas the smaller clusters adopt planar geometries and obtain satisfactory agreement between experimental and calculated vertical ionization potentials (VIPs).

Our theoretical study on small neutral cesium clusters is mainly motivated by the lack of published accurate electronic properties such as the dipole polarizability and also by the shortcomings of previous models used.[74] The only theoretical disquisition on the static electric-dipole polarizability of cesium clusters[45] dates back to 1989, where only Cs_4 and Cs_6 clusters were considered. Moreover, independent of the model used to describe the bonding in clusters, one of the prime objectives is to find the geometrical arrangement of atoms that corresponds to the lowest potential energy on the potential-energy surface, i.e., the most stable (global minimum) structure. In the work by Lai *et al.*,[73] an unbiased search for the global minimum structure was undertaken; however, we believe that the employment of empirical potentials based on bulk data will essentially favor a maximum number of close atom-atom contacts and thus compact structures. For example, we expect that Cs_3 undergoes a Jahn-Teller distortion like all the other lighter alkali metals,[76] which is a manifestation of the importance of many-body effects.[74] Furthermore, we are interested in the convergence of electronic properties for clusters to the bulk limit.

In this paper we present a concise theoretical study of predicted global minimum structures of neutral cesium clusters up to 20 atoms by employing our density-functional-based genetic algorithm code and discuss the static electric-dipole polarizability together with other electronic and geometric properties as a function of cluster size. Furthermore, we provide solid-state calculations of cesium to verify the validity of our extrapolated value for bulk properties of cesium.

II. COMPUTATIONAL METHODS

The predicted low-spin global minima—all structures are singlet states for even-numbered clusters and doublet states for odd-numbered ones—of cesium clusters (Cs_{2-20}) were obtained utilizing our genetic algorithm code as described in detail in Ref. 77. The initial populations of clusters with up to six atoms were generated randomly, whereas those for the larger ones, typically ranging from 10 to 12 different structures, consisted of both randomly generated structures and predicted low-lying minimum structures of sodium clusters from the literature.[33,35] The minimum-energy difference δ_iV was set to 0.002 eV. Shortest ($d_{\min}$) and longest ($d_{\max}$) bond distances were fixed at 2.8 and 8–10 Å, respectively, and the mutation probability was set to 10%. All structures in the initial population were relaxed into their nearest local minimum using local spin-density approximation DFT according to Slater's exchange and the correlation functional of Vosko, Wilk, and Nusair (SVWN) with the Los Alamos minimum basis set and corresponding shape-consistent scalar-relativistic pseudopotential for cesium as implemented in the GAUSSIAN03 program package.[78]

As this search is very computer time intensive for the larger clusters, in general, the only termination criterion for the genetic algorithm was 150 mating and local minimization steps for clusters up to ten atoms and 100 steps for the remainder. Despite this fixed termination criterion we are quite confident that we have found global and low-lying local minima with a very high probability. This is so because there is clear evidence that each respective population is converging toward the predicted global minimum structures of this work and because we tested our genetic algorithm approach for copper nonamer isomers and obtained the same geometric and energetic patterns for isomers for numerous runs of the algorithm.[77] Furthermore, our approach resulted in a number of other and more stable isomers of small tin clusters.[79]

Depending on the cluster energy distribution, the energetically lowest-lying six to ten isomers obtained by these means were then further optimized using the LANL2DZ valence basis set and corresponding pseudopotentials. Four to six of the energetically lowest-lying stationary points obtained by this procedure were then further optimized using the more accurate Stuttgart valence basis set ($8s8p2d1f$) derived from Ref. 48 together with a small-core energy-consistent scalar relativistic pseudopotential for cesium, which leaves the innermost 46 electrons in the core. Finally, a harmonic vibrational analysis was performed for all clusters in order to discriminate between minima and possible transition states on the potential-energy surface. All reported properties were calculated based on these structures. For the exchange-correlation potential, the generalized gradient approximation (GGA), according to the parametrization suggested by Becke[80] and Perdew[81] (BP86), was applied in a self-consistent fashion. No symmetry constraints were applied during the optimization procedure.

In Fig. 1, calculated atomic polarizabilities for a variety of different exchange and correlation functionals are compared to the experimental value of 59.43 ± 0.08 Å^3 by Amini and Gould[11] and to a recent accurate coupled-cluster [CCSD(T)] calculation employing a relativistic Douglas-Kroll-Hess (DKH) transformation (58.69 Å^3).[48,82] Here we used a variety of different functionals, i.e., the local spin-density approximation (LSDA) using Slater's exchange and the SVWN correlation functional; a later variant of this local correlation

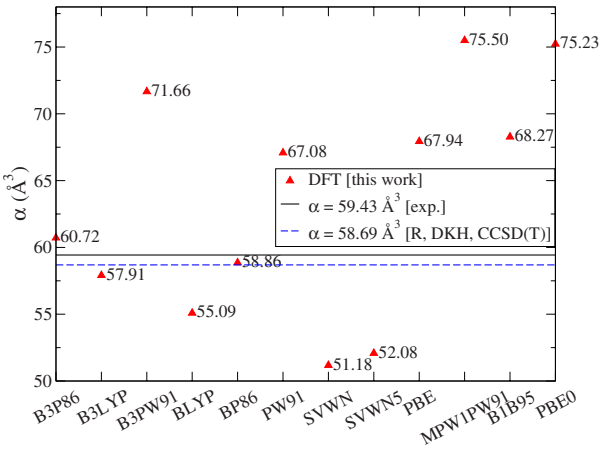

FIG. 1. (Color online) Static electric-dipole polarizabilities of the cesium atom as a function of different exchange-correlation functionals and compared to experimental (Ref. 11) and calculated coupled-cluster (Ref. 48) values.

functional (SVWN5); gradient-corrected functionals such as Becke's 1988 exchange functional; the correlation functional of Lee, Yang, and Parr (BLYP) including both local and nonlocal terms; Becke's 1988 exchange functional and the correlation functional of Perdew (BP86); Perdew and Wang's 1991 (PW91) exchange and correlation functional; the 1996 exchange functional of Perdew, Burke, and Ernzerhof (PBE) and respective correlation functional; hybrid functionals containing exact exchange such as Becke's 1996 functional (B1B95); a similar hybrid functional as implemented by Adamo and Barone employing modified Perdew-Wang exchange and Perdew-Wang 91 correlation (MPW1PW91); the 1997 functional of Perdew, Burke, and Ernzerhof (PBE0); Becke's 1993 functionals using the nonlocal correlation provided by Lee, Yang, and Parr (B3LYP); the nonlocal correlation provided by Perdew in 1986 (B3P86); and the nonlocal correlation provided by Perdew and Wang in 1991 (B3PW91).[78] Clearly, the BP86 exchange-correlation potential within the GGA, combined with the extensive Stuttgart valence basis set and pseudopotential for cesium, gives excellent agreement with the aforementioned experimental and calculated results.

For the bulk calculations, we performed density-functional calculations using a plane-wave basis within the projector augmented wave (PAW) method[83] as implemented in the Vienna *ab-initio* Simulation Package (VASP).[84,85] Unfortunately, Becke's 1988 exchange functional and the correlation functional of Perdew (BP86) is not implemented in VASP and we therefore modeled the exchange-correlation contribution to the total energy using the PBE and PW91 functionals.[86,87] For comparison, some calculations were carried out within the local-density approximation (LDA).[88] The plane-wave cutoff for the wave-function expansion is 400 eV. The Brillouin zone was sampled by $6\times6\times6$ k points. For all solid-state calculations we adopted the experimentally found crystal structure of bulk cesium, which is body-centered cubic (bcc, $Im3m$). The crystal properties such as the lattice constant a, cohesive energy E_{coh}, and bulk modulus B were obtained by fitting the total-energy values for different volumes of the crystal to the Murnaghan equation of state.[89]

III. RESULTS AND DISCUSSION

A. Structural data

Figure 2 depicts the predicted global minimum structures of neutral cesium clusters with up to 20 atoms and their energetically close-lying isomers. As can be seen from the relative energies (see Table I) of the respective isomers, a clear distinction between the global minimum and low-lying isomers cannot always be made. The relative total-energy difference between the cesium hexamer isomers (Cs_{6_0} and Cs_{6_1}), for instance, adds up to only 0.002 eV, which is clearly too small to appoint either of them as the global minimum structure of Cs_6. It is interesting that for the clusters Cs_3–Cs_6 linear structures are true local minima, with alternating bond lengths for the Cs_4, Cs_5, and Cs_6 isomers. While the relative energy difference for the linear tetramer to the parallelogram (C_s) is a marginal 0.05 eV that of the linear hexamer compared to the tricapped triangle (D_{3h}) is already 0.4 eV. The transition from planar [two-dimensional (2D)] to 3D structures is ambiguous but most probably occurs at cluster size 7. This is so, because the pentagonal bipyramid (Cs_{7_0}, D_{5h}) is energetically more stable than the bicapped planar trapezoidal structure (Cs_{7_2}, C_s) by 0.305 eV. In contrast, for the pentamer, the isosceles trapezoid (Cs_{5_0}, C_{2v}) is energetically favored by 0.238 eV over the trigonal bipyramid (Cs_{5_2}, D_{3h}). The relative energy difference between the tricapped triangle (Cs_{6_0}, D_{3h}) and the pentagonal pyramid (Cs_{6_1}, C_{5v}) is, however, negligible.

Thus, in the light of relative energy differences, cesium pentamers formed in an experiment should be mostly planar, while the heptamers should be mostly three dimensional. For the hexamer, without consideration of any kinetically driven factors, an almost equal mixture of both 2D and 3D structures should be expected. For comparison, the global minimum structure of Li_6 in the singlet spin state is reported to be 3D in Refs. 16, 18, 22, and 23 and 2D in Ref. 19. Judging from the dip in the trend of measured isotropic polarizabilities per atom as a function of cluster size, Li_6 most probably adopts a 3D structure[15] (see Fig. 3). The sodium hexamer is reported to be 3D in Refs. 27, 28, 30, 31, and 33–35. This prediction is confirmed experimentally in Ref. 3, where, compared to smaller clusters, a clear decrease in the polarizability per atom is observed for the hexamer as one expects for a more compact structure. This decrease is, however, not obvious in Ref. 15. Potassium hexamers are also predicted to adopt the pentagonal pyramidal (3D) structure.[3,39] It should be noted that the theoretical studies exhibit a trend in which the relative energy difference between the tricapped triangle (2D) and the pentagonal pyramid (3D) isomers of alkali clusters diminishes with increasing nuclear charge Z. Thus, we infer that there is a shift toward higher nuclearity in the transition from 2D to 3D down the group of the alkali clusters and that the tricapped triangular and pentagonal pyramidal hexamers become more and more degenerate in energy down this group.

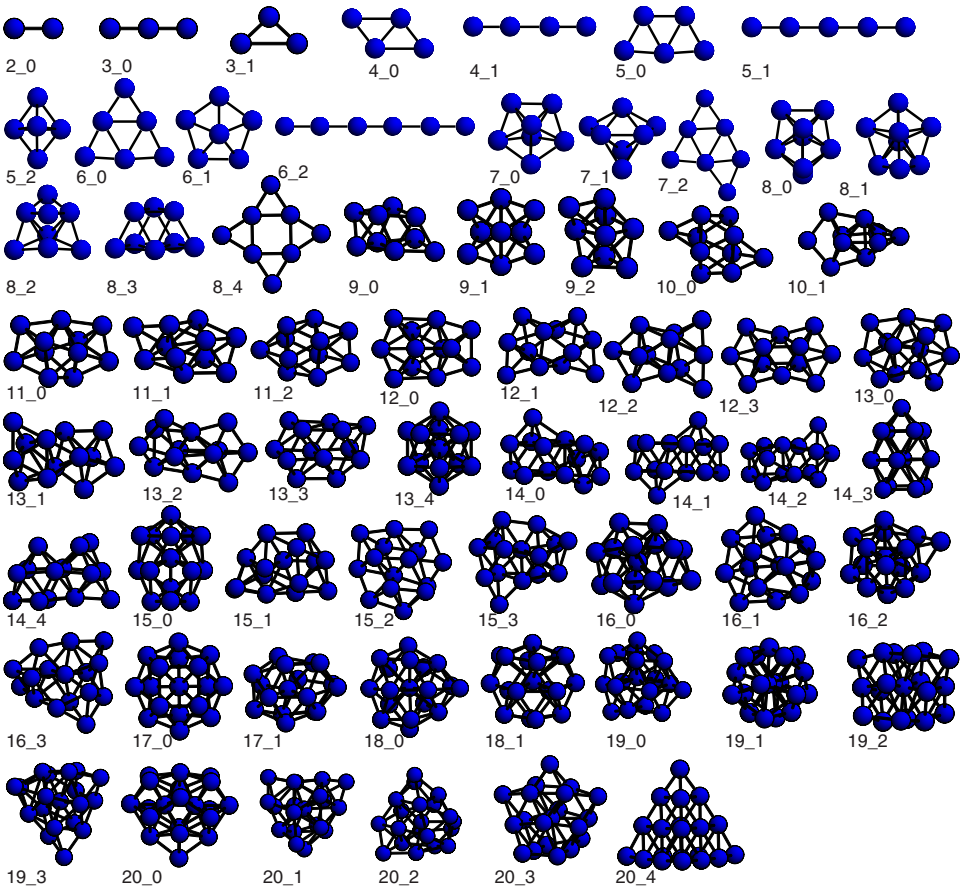

FIG. 2. (Color online) Predicted global minimum and lowest-energy isomers of Cs_{2-20} ordered (from left to right and top to bottom) by increased size and energy. The cluster n_m denotes the mth energetic isomer with n atoms.

As mentioned before, a clear appointment of the energetically most stable isomer is not always possible for most of the isomers presented here. Nevertheless, we compare our cesium morphologies with recent theoretical studies[72,73,75] and point out that in Ref. 75 apparently no vibrational analysis was undertaken. We optimized three of these rather unusual structures together with a vibrational analysis, which revealed that such structures (namely, Cs_{4a}, Cs_{8a}, and Cs_{8b} in Ref. 75) are not true minima. Nevertheless, we report the same predicted global minima for the trimer, pentamer, heptamer, and decamer as in Ref. 75. In Ref. 73 a combined search for global minimum structures was undertaken utilizing a genetic algorithm and a basin hopping method. However, they report the global minimum of the alkali tetramers and pentamers, and even those for the tetravalent lead tetramer and pentamer, as a tetrahedron and a trigonal bipyramid, respectively. Our geometry optimization of the Cs_4 in tetrahedral symmetry (T_d) leads to distortions, due to a first-order Jahn-Teller effect, into its geometric analogons with C_{2v} and C_s symmetries. Any possible 3D geometry in other electronic states (triplet or quintet spin states) for Cs_4 lie higher in energy than our parallelogram (Cs_{4_0}) by at least 0.2 eV. We also find that the flat Cs_{5_0} is more stable than the triangular bipyramid (Cs_{5_2}) by 0.238 eV. Note that the singlet state of the octahedral Cs_6 structure (T_d) is not a local minimum and that the distorted variants in the D_{4h} point group are less stable than the global minimum Cs_{6_0} isomer by more than 0.5 eV using the Los Alamos pseudopotentials and corresponding double zeta valence basis sets.[78] We therefore point out that the proposed icosahedral-like growth pattern for alkali-metal clusters[73] is, at least for small clusters, incorrect at the DFT level. Although key isomers such as the Cs_{13_4} (icosahedron), Cs_{19_1} (double icosahedron), and Cs_{20_0} (capped double icosahedron) are found to be energetically low-lying isomers in this work, there are, however, asymmetric isomers that have almost the same energetic stability as these highly symmetrical structures. For instance, the asymmetric Cs_{13_0} is more stable than the icosahedron Cs_{13_4} by 0.112 eV. Note that the tetrahedral Cs_{20} cluster (structure Cs_{20_4} in Fig. 2) is only a local minimum, 0.28 eV above the global minimum in contrast to Au_{20}.[90] These results clearly demonstrate that the many-body potential used in Ref. 73 favors compact structures, similar to Lennard-Jones potentials, for small clusters and does not represent the best approach for the search of global minimum structures for metal clusters. In a recent study, it was found that for metallic or covalent interactions in small clusters, empirical potentials such as the Gupta potential fail to describe the cluster's geometry accurately as opposed to *first-principles* wave-function- and density-functional-based methods.[74] Since the parameters of such potentials are optimized to reproduce certain bulk material properties, their application to small clusters remains questionable.

B. Electronic properties

The main results in this work concerning the static response properties in conjunction with selected electronic

TABLE I. Nearest-neighbor distances d, relative energies ΔE, vertical ionization potentials (VIP), vertical electron affinities (VEA), and cohesive energies E_{coh} (dissociation energies per atom, not corrected for zero-point vibration) of the lowest-energy Cs_n cluster isomers $2 \leq n \leq 20$. The notation for the different structures is shown in Fig. 2. The BP86 functional was used throughout.

Cluster	d (Å)	ΔE (eV)	VIP (eV)	VEA (eV)	E_{coh} (eV/n)	Cluster	d (Å)	ΔE (eV)	VIP (eV)	VEA (eV)	E_{coh} (eV/n)
1_0			4.053	0.576		12_4		0.142	2.945	1.085	0.352
2_0	4.695		3.855	0.602	0.198	13_0	5.137	0.000	2.901	1.119	0.367
3_0	4.925	0.000	3.505	0.987	0.192	13_1		0.024	2.914	1.112	0.365
3_1		0.006	3.375	0.809	0.190	13_2		0.058	2.940	1.120	0.362
4_0	5.853	0.000	3.296	0.811	0.234	13_3		0.061	2.980	1.153	0.362
4_1		0.050	3.402	1.034	0.221	13_4		0.122			0.357
5_0	5.080	0.000	3.264	0.983	0.263	14_0	5.131	0.000	2.985	1.004	0.374
5_1		0.209	3.251	1.240	0.222	14_1		0.010	2.947	0.997	0.373
5_2		0.238	3.252	0.807	0.216	14_2		0.030	2.954	1.009	0.372
6_0	5.075	0.000	3.383	0.837	0.299	14_3		0.064	2.919	1.046	0.369
6_1		0.002	3.347	0.844	0.299	14_4		0.095	2.935	1.059	0.367
6_2		0.400	3.182	1.279	0.232	15_0	5.121	0.000	2.929	1.125	0.380
7_0	5.197	0.000	3.236	0.910	0.330	15_1		0.092	2.900	1.131	0.374
7_1		0.096	3.209	0.911	0.317	15_2		0.099	2.922	1.161	0.373
7_2		0.305	3.077	1.039	0.287	15_3		0.163	2.954	1.179	0.369
8_0	5.072	0.000	3.281	0.783	0.353	16_0	5.007	0.000	2.941	1.177	0.386
8_1		0.075	3.196	0.837	0.344	16_1		0.035	2.906	1.173	0.384
8_2		0.089	3.291	0.781	0.342	16_2		0.046	2.956	1.184	0.383
8_3		0.096	3.211	0.861	0.341	16_3		0.103	2.962	1.113	0.380
8_4		0.471	3.047	1.060	0.294	17_0	5.205	0.000	3.064	1.291	0.396
9_0	5.110	0.000	3.077	1.023	0.343	17_1		0.020	2.953	1.195	0.395
9_1		0.010	2.908	0.918	0.342	18_0	5.107	0.000	3.003	1.161	0.403
9_2		0.019	2.913	0.901	0.341	18_1		0.017	3.004	1.188	0.402
10_0	5.151	0.000	2.995	0.954	0.349	19_0	5.183	0.000	2.935	1.252	0.405
10_1		0.001	2.979	0.924	0.349	19_1		0.035	2.834	1.170	0.403
11_0	5.149	0.000	2.993	1.102	0.356	19_2		0.046	2.970	1.316	0.403
11_1		0.030	2.967	1.071	0.353	19_3		0.053	2.920	1.251	0.402
11_2		0.035	2.976	1.055	0.353	20_0	5.022	0.000	2.801	1.162	0.408
12_0	5.124	0.000	2.995	1.056	0.364	20_1		0.004	2.962	1.070	0.408
12_1		0.039	3.032	1.016	0.361	20_2		0.140	2.893	1.077	0.401
12_2		0.072	3.022	0.995	0.358	20_3		0.217	2.871	1.117	0.397
12_3		0.099	3.057	1.001	0.356	20_4		0.275	2.994	1.095	0.394

structure properties of small cesium clusters are collected in Table II. Structural properties and vertical ionization potentials and vertical detachment energies are displayed in Table I.

As expected, the mean (isotropic) polarizability per atom of a clusters as a function of size approaches the bulk limit from above, which is also the case for measured and calculated lithium and sodium polarizabilities (see Fig. 3). This stems from the stabilizing bonding orbitals for even clusters which form the conduction band in the solid.[91] While the deviation from the classical bulk limit[92] of Cs_{20} is about 26% that of Li_{20} and Na_{20} are about 42 and 40%, respectively. Hence, cesium clusters approach their bulk polarizability value faster than the corresponding lithium and sodium clusters. The atomic polarizability of cesium (58.85 Å^3) is far greater than those of lithium (24.4 Å^3),[16] sodium (24.12 Å^3),[26] potassium (43.51 Å^3),[49] and rubidium (47.41 Å^3).[49] This is qualitatively attributed to the stronger screening of the valence s electrons down the group and to relativistic effects that are not yet large enough to change this trend. As in the case of lithium and sodium clusters, there is a marked decrease in polarizability from the cesium atom to its dimer. The two energetically lowest-lying isomers of trimeric cesium (Cs_{3_0} and Cs_{3_1}) show higher polarizabilities than the cesium atom. Cs_{3_2} is more compact than the aforementioned isomers, less polarizable, and hence confirms the strong geometrical dependency of the polarizability. The transition from 2D to 3D structures in cesium results also in a significant decrease in polarizabilities [compare values for (2D) Cs_{6_0} and (3D) Cs_{6_1}]. This transition is not that evident

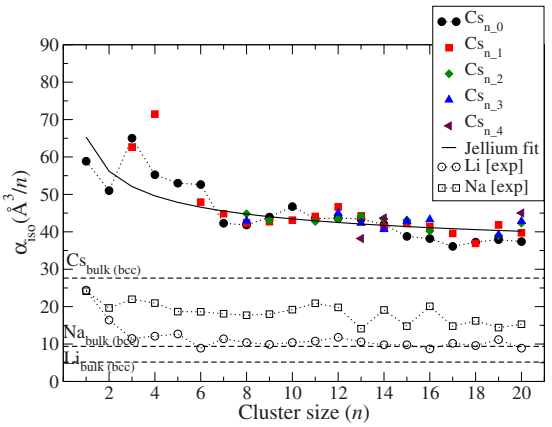

FIG. 3. (Color online) Isotropic static electric-dipole polarizabilities per atom of Cs_n clusters as a function of cluster size compared to the classical bulk value bcc Cs. The solid black curve represents the prediction for the classical metallic sphere. The measured polarizabilities of Li_n (extracted from Refs. 15 and 16) and Na_n (extracted from Refs. 15 and 26) clusters are also shown and compared to their classical bulk bcc polarizabilities.

in the measured data for sodium in Ref. 15 but is significant in the early work of Knight *et al.*[3] and occurs for lithium at cluster size 6.[15] Interestingly, the energetically lowest-lying isomers (Cs_{n_0}) also exhibit in most cases the smallest isotropic polarizabilities per atom.

The solid curve in Fig. 3 corresponds to the polarizability calculated for a finite metallic sphere according to the jellium model in the spillout approximation fitted to our Cs_{n_0} data and agrees nicely for the heavier clusters with the calculated values. From this fit, the spillout of the electrons from the surface of the metallic sphere adds to 0.96 Å and a Wigner-Seitz radius of 3.07 Å is obtained. This agrees very nicely with the Wigner-Seitz radius (r_{WS}) derived from crystallographic data of bcc Cs as follows:

$$r_{WS} = \sqrt[3]{\frac{3}{4\pi N}}a = 3.02 \text{ Å} = \sqrt[3]{\alpha_{iso}}. \quad (1)$$

Here, a denotes the lattice constant, N the number of atoms in bcc cesium, and α_{iso} the isotropic polarizability defined as the average of the trace of the polarizability tensor,

$$\alpha_{iso} = \mathrm{Tr}(\alpha)/3. \quad (2)$$

For lithium and sodium clusters it is also found that the jellium picture nicely describes the evolution of the polarizability per atom with increasing cluster size (Li: r_{WS} =1.75 Å and the spillout parameter δ=0.75 Å; Na: r_{WS} =2.12 Å and δ=0.69 Å).[16] Despite the fact that the jellium model in the spillout approximation predicts on average the trend of the polarizability per atom as a function of the cluster size, it can of course not account for the more interesting quantum effects.

The anisotropy per atom (α_{aniso}) is obtained from the diagonal form of the polarizability tensor,

$$\alpha_{aniso} = \left\{\frac{1}{2}[3\ \mathrm{Tr}(\alpha^2) - (\mathrm{Tr}\ \alpha)^2]\right\}^{1/2} = \left\{\frac{1}{2}[(\alpha_{xx}-\alpha_{yy})^2 + (\alpha_{xx}-\alpha_{zz})^2 + (\alpha_{yy}-\alpha_{zz})^2]\right\}^{1/2}, \quad (3)$$

and is given in Table II. α_{aniso} increases rapidly from monomeric to trimeric cesium and then decreases toward Cs_8. It is worthy to mention the difference in anisotropies for the Cs_3 isomers, where the linear structure (Cs_{3_0}) shows an anisotropy that is almost twice as large as that of the isosceles triangle (Cs_{3_1}). The transition to 3D structures (Cs_6-Cs_7) is followed by a significant decrease in α_{aniso}. The anisotropy is per definition strongly dependent on the geometric structures of the respective isomers and approaches zero for spherically shaped isomers. The general decreasing trend in α_{aniso} for clusters $10 \le n \le 20$ also underlines the fact that their evolution tends toward more compact and spherically shaped clusters.

As depicted in Fig. 4, the VIPs decrease and the VEAs increase toward the work function (W_f) of bulk cesium, and the evolution of both properties with respect to $n^{-1/3}$ can be approximated satisfyingly by linear regressions according to $G(n) = 1.93 + A_0 n^{-1/3}$. Here, $G(n)$ denotes the VIPs and VEAs as functions of cluster size and 1.93 eV is the work function W_f.[93] It should be noted that the BP86 functional is not the best functional to calculate atomic ionization potentials and electron affinities for metals. We find that BP86 overestimates the experimental atomic ionization potential for cesium (3.894 eV) (Ref. 94) by around 4% and its electron affinity (0.472 eV) (Refs. 60 and 67) by around 22%. These deviations are much smaller for the PBE0, B3PW91, and MPW1PW91 functionals. However, the choice of the BP86 functional was not founded on the reproduction of the atomic experimental ionization potential or electron affinity, but on the accurate reproduction of the atomic polarizability. Moreover, the interpretation of photoionization spectra as well as photoelectron spectra of clusters is far from straightforward due to uncertainties in the temperatures of the clusters, Franck-Condon factors, isomerization, and fragmentation processes.[64] Our calculated VIPs are, after scaling, in good agreement with the available experimental data [experimental references for Cs_1,[94] Cs_2,[57] and Cs_{9-15} (Ref. 65)].

We observe a clear even-odd oscillation for the VEAs, where the closed-shell clusters show smaller electron affinities due to the electron pairing effect. The calculated VEAs of Cs_2 and Cs_3 are in good agreement with experimental photoabsorption spectra data obtained for Cs_2^- (0.511 eV) and Cs_3^- (0.987 eV).[61] Experimental photoabsorption spectra for Cs_4 to Cs_9 were measured by Martin and co-workers.[62] However, the emphasis of that work was put on the spectral region 1.3–1.7 eV and, hence, no conclusion can be drawn upon the first electron affinities.

The so-called disproportionation energy (second difference in cluster energy) defined as

$$\Delta_2 E_n(n) = E_{n+1} - 2E_n + E_{n-1}, \quad (4)$$

where E_n is the calculated total electronic energy of the cluster with n atoms, is displayed in Fig. 5. $\Delta_2 E_n$ represents the

TABLE II. Calculated static response and electronic structure properties of low-spin DFT-optimized Cs_n clusters. The second difference in cluster energy is denoted by $\Delta_2 E_n$ and $\Delta\epsilon$ stands for the HOMO-LUMO gap. The mean static polarizability per atom α_{iso} and the polarizability anisotropy α_{aniso} per atom were calculated analytically. The absolute value of the dipole moment is denoted by μ. The notation $/n$ implies that the value is given per atom. The BP86 functional was used throughout.

Cluster	$\Delta_2 E_n$ (eV)	$\Delta\epsilon$ (eV)	α_{iso} (Å$^3/n$)	α_{aniso} (Å$^3/n$)	μ (D)	Cluster	$\Delta_2 E_n$ (eV)	$\Delta\epsilon$ (eV)	α_{iso} (Å$^3/n$)	α_{aniso} (Å$^3/n$)	μ (D)
1_0		0.469	58.85	0.0	0.0	12_4		0.210	41.87	15.63	0.507
2_0	0.214	0.760	51.00	38.85	0.0	13_0	−0.074	0.186	43.41	22.61	0.191
3_0	−0.178	0.314	65.01	84.73	0.0	13_1		0.206	44.26	28.90	0.281
3_1		0.337	56.53	46.15	0.120	13_2		0.214	44.20	28.29	0.544
4_0	−0.022	0.464	55.241	56.94	0.0	13_3		0.197	42.35	20.58	0.192
4_1		0.442	71.47	114.1	0.0	13_4		0.229	38.21	0.20	0.0
5_0	−0.097	0.291	52.99	44.89	0.033	14_0	0.008	0.416	41.96	19.95	0.161
5_1		0.494	89.91	170.4	0.0	14_1		0.390	41.28	18.78	0.126
5_2		0.346	49.09	8.73	0.0	14_2		0.383	43.44	22.59	0.887
6_0	−0.042	0.716	52.64	38.60	0.0	14_3		0.288	40.66	21.17	0.605
6_1		0.585	47.95	29.77	0.056	14_4		0.337	43.69	21.66	0.523
6_2		0.314	98.24	199.5	0.0	15_0	−0.015	0.206	38.77	11.56	0.312
7_0	0.007	0.340	42.29	14.98	0.0	15_1		0.213	42.21	20.16	0.418
7_1		0.325	44.84	15.00	0.0	15_2		0.207	43.11	20.99	0.259
7_2		0.266	57.30	52.92	0.226	15_3		0.213	42.88	17.86	0.862
8_0	0.251	0.633	41.83	12.67	0.0	16_0	−0.075	0.195	38.18	11.37	0.423
8_1		0.518	42.36	12.76	0.119	16_1		0.195	41.41	17.30	0.193
8_2		0.713	44.83	0.0	0.119	16_2		0.224	40.19	12.57	0.157
8_3		0.522	42.92	13.21	0.479	16_3		0.224	43.28	18.76	0.638
8_4		0.356	57.96	47.70	0.0	17_0	0.025	0.207	36.10	6.73	0.0
9_0	−0.144	0.250	43.94	24.90	0.210	17_1		0.207	39.56	13.66	0.281
9_1		0.219	42.69	16.11	0.417	18_0	0.089	0.327	37.24	8.27	0.444
9_2		0.236	43.07	16.22	0.799	18_1		0.296	36.91	5.95	0.250
10_0	−0.013	0.323	46.74	31.57	0.0	19_0	−0.029	0.210	37.91	5.28	0.227
10_1		0.347	43.13	24.06	0.235	19_1		0.173	41.82	1.34	0.018
11_0	−0.036	0.210	43.51	28.27	0.332	19_2		0.164	39.02	5.96	0.0
11_1		0.220	44.11	28.44	0.239	19_3		0.204	39.17	7.45	0.607
11_2		0.225	42.75	25.62	0.849	20_0		0.167	37.39	7.19	0.178
12_0	0.059	0.312	43.66	26.75	0.423	20_1		0.473	39.73	1.28	0.436
12_1		0.423	46.63	29.96	0.031	20_2		0.420	42.31	3.64	0.260
12_2		0.419	43.50	23.50	0.382	20_3		0.473	42.82	5.81	0.949
12_3		0.442	45.01	31.47	0.0	20_4		0.533	45.04	0.0	0.0

relative stability of a cluster with n atoms in comparison to clusters with $n+1$ and $n-1$ atoms, and consequently a peak in $\Delta_2 E_n$ indicates that the cluster with size n is very stable, i.e., a magic cluster. With the exception of Cs_6 and Cs_{16}, a clear odd-even oscillation is present in the disproportionation energy, where due to the electron pairing effect, even-sized clusters are more stable than odd ones. While the deviant behavior of Cs_6 from the odd-even oscillation is due to the transition from 2D to 3D structures, the low stability of Cs_{16} with respect to its neighbors is peculiar. Perhaps there exists a more stable isomer which we did not find. The disproportionation energy shows that clusters with $n=2$, 8, 12, and 18 have particularly stable configurations. The driving force behind the stability of Cs_2, Cs_8, and Cs_{18} is electronic shell closure described by the jellium model.[1]

The electron pairing effect also explains the oscillatory trend in the highest occupied molecular orbital (HOMO)-lowest unoccupied molecular orbital (LUMO) gaps ($\Delta\epsilon$), which is depicted in Fig. 6. Odd- (even-) sized clusters have an odd (even) number of 6s valence electrons, and the HOMO is singly (doubly) occupied. The binding energy of a valence electron in a cluster of even size is therefore larger than that of an odd one, thus exhibiting a larger gap. Comparison between Figs. 5 and 6 reveals a resemblance between cluster stability and HOMO-LUMO gaps. Clusters that show higher stability ($n=2,8,12,18$) also exhibit large HOMO-LUMO gaps. Cs_6 is an exception to that, exhibiting a large gap, but no peak in the second difference in cluster energy. This missing peak is due to the transition from planar to three-dimensional structures. HOMO-LUMO gaps are most

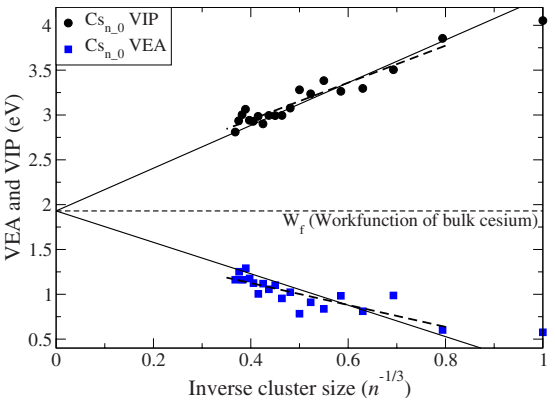

FIG. 4. (Color online) Vertical electron affinities and vertical ionization potentials of cesium clusters as functions of inverse cluster size ($n^{-1/3}$). The continuous lines denote the evolution of both properties as constrained linear regressions according to $G(n)=1.93+2.38x$ and $G(n)=1.93-1.75x$, where 1.93 denotes the work function of bulk cesium and $x=n^{-1/3}$ (Ref. 93). The dashed lines, $G(n)=2.12+2.06x$ and $G(n)=1.61-1.22x$, denote unconstrained linear regressions for Cs_{2-20}.

important for the discussion of the onset of metallic behavior at certain cluster sizes. While the clusters investigated here are still too small for a detailed analysis, an extrapolation of only the odd-sized (open-shell)-type clusters suggests an onset at around Cs_{40}, but this value has to be taken with care, e.g., compare the discussion about the onset of metallicity for mercury clusters.[95,96]

No obvious relation between HOMO-LUMO gaps and dipole moments can be found. For most of the germanium clusters ($n=11-25$), a close relation between these two properties was found, where a large HOMO-LUMO gap corresponds to a large dipole moment.[97] Our calculated dipole moments are listed in Table II. There is also no stringent relationship between dipole moments and the isotropic polarizability or its anisotropy. In general, clusters with near-spherical structures have smaller dipole moments compared to those exhibiting distorted prolate or oblate structures.

Nearest-neighbor distances, which as opposed to average bond distances exclude surface effects, of the energetically most stable isomers are listed in Table I. Abrupt increases are obtained for transitions from one dimensional (1D) to 2D

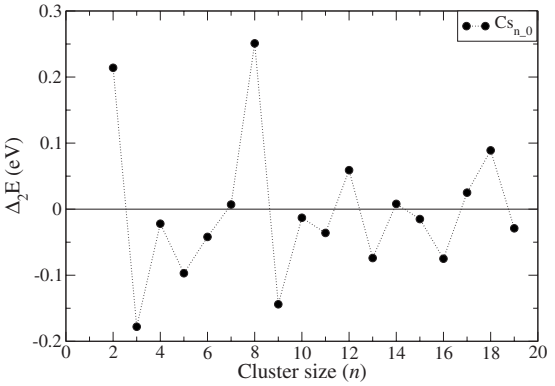

FIG. 5. Second difference in cluster energy ($\Delta_2 E$) as a function of cluster size n.

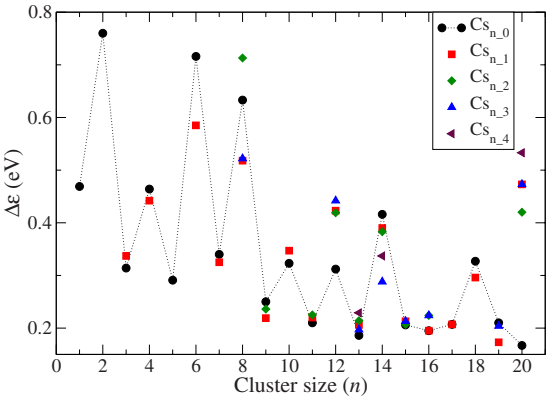

FIG. 6. (Color online) HOMO-LUMO gaps ($\Delta\epsilon$) of cesium clusters as a function of cluster size n.

and from 2D to 3D. Our calculated cesium dimer bond length (4.695 Å) agrees nicely with the experimental value (4.65 Å),[56,58] and in general, the nearest-neighbor distances approach the experimental value for the shortest equilibrium interatomic distance in bulk bcc cesium (5.318 Å) from below.

The cohesive energies, defined as $E_{coh}=[nE(Cs_1)-E(Cs_n)]/n$, where $E(Cs_1)$ denotes the calculated total electronic energy of the cesium atom, are reported in Table I and in Fig. 7, where the cohesive energy as a function of inverse cluster size ($n^{-1/3}$) is extrapolated toward its bulk value. Due to the small relative energy differences between the respective isomers, the cohesive energy is relatively independent of the isomeric structure. We obtain for the most stable isomers an approximately linear increase in E_{coh} from Cs_3 to Cs_8, followed by a decrease toward Cs_9, and a further linear increase, with a considerably smaller slope, for Cs_9-Cs_{20}. The onset of this change is considerable, correlates strongly with the HOMO-LUMO gaps, and indicates the start toward metallicity. The cohesive energy of Cs_{20} is 0.408 eV, which is about 50% of its experimental bulk value (0.83 eV).[98] We should also mention that our calculated cohesive energies for

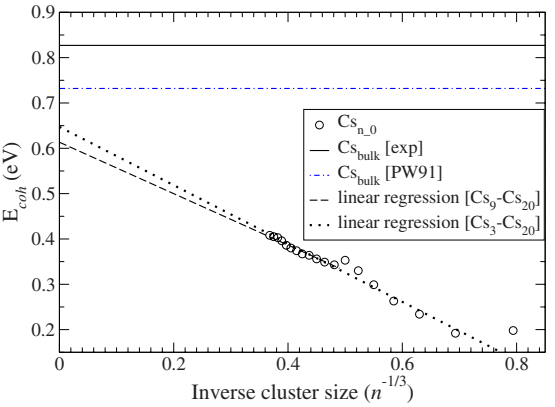

FIG. 7. (Color online) The calculated cohesive energies of cesium clusters as a function of inverse cluster size. Two sets of cluster values are extrapolated and compared to the observed (0.83 eV) (Ref. 98) and calculated (0.732 eV) (this work) cohesive energy of bulk cesium. Further calculated cohesive energies are listed in Table III.

TABLE III. Calculated lattice constants a in Å, bulk moduli B in GPa, and cohesive energies E_{coh} in eV for bulk cesium (bcc) at the DFT level compared to experimental data.

Method	a	B	E_{coh}	Reference
LDA	5.783	2.430	0.883	This work
PBE	6.156	2.245	0.728	This work
PW91	6.142	2.202	0.732	This work
$X(\alpha)$	6.216	1.4	0.776	99
$X(\alpha)$	6.083	1.8	0.830	99
LDA	6.027	2.20		100
Expt.	6.141	2.15	0.83	91, 94, and 98

the clusters are about 30% larger than those published by Maity and co-workers[75] but with similar trends. In comparison, the cohesive energy of Na_{20} is about 55% smaller than the experimental cohesive energy of bulk sodium [1.13 eV (Ref. 99)].[33]

Considering the fact that Cs_{20} is far away from the bulk limit, the linear extrapolations in Fig. 7 yield bulk cohesive energies that deviate by only 25% from the experimental value for bulk cesium. It should be noted, however, that different DFT functionals will characterize the binding situations differently and can therefore result in quite different cohesive energies. For Li_{10}, for instance, the local-density approximation yields a cohesive energy of 1.38 eV and the gradient corrected approaches (BP86) a value of 1.18 eV.[23] Chermette and co-workers[22] also, utilizing the BP86 functional, report the cohesive energy of Li_{10} to be 0.84 eV and that of the biggest cluster they investigated, Li_{13}, to be 0.88 eV. They also report cohesive energies for various DFT functionals. The experimental cohesive energy of bulk Li is reported to be 1.65 eV.[98] The observed cohesive energy of bulk cesium (0.83 eV) (Ref. 98) is confirmed by Averill's calculations based on the statistical ($X\alpha$) exchange-correlation approximation[99] and our calculations, as presented in Table III. For the PBE and PW91 functionals, we find excellent agreement between theory and experiment for the lattice constant and good agreement for the bulk modulus, whereas the local-density approximation slightly overbinds, which also results in an overestimated bulk modulus.[100]

Finally, we estimate the zero-point vibrational energy for bulk cesium. From the Debye model we obtain the well-known relation between the Debye temperature Θ_D and the zero-point vibrational energy E_{ZPVE},[101]

$$E_{ZPVE} = \frac{9}{8} k_B \Theta_D. \quad (5)$$

From the estimated Debye temperature of 38 K for cesium[102,103] we obtain a zero-point vibrational energy of 0.004 eV. By means of extrapolation from our zero-point vibrational values for our clusters, we find in accordance with the Debye model a rather small zero-point vibrational energy per atom of 0.006 eV.

IV. CONCLUSION

We are confident that our density-based systematic search for the global minimum structures of cesium clusters up to 20 atoms resulted in the most stable isomers published so far. The transition from two- to three-dimensional structures is ambiguous since the tricapped triangular and pentagonal pyramidal hexamer isomers exhibit almost identical total electronic energies. Comparing this finding with other work on alkali-metal clusters lets us infer that there is a slight shift toward higher nuclearity in the transition from two- to three-dimensional structures down the group of alkali clusters. A proposed icosahedral-like growth pattern is shown to be incorrect for the cluster size regime discussed here. Both, the observed and calculated static electric-dipole polarizabilities of atomic cesium are excellently described by the BP86 functional. The evolution of the polarizability per atom with increasing cluster size is nicely described by the jellium model and it is found that, in general, the most stable isomers also exhibit the lowest polarizability. From its anisotropy it is inferred that the clusters adopt more compact and spherical shapes as the cluster size increases. We obtain good agreement between observed and calculated ionization potentials and electron affinities and report an odd-even behavior for the vertical electron affinities and HOMO-LUMO gaps as a function of cluster size. The onset of metallic character, based on diminishing HOMO-LUMO gaps, is suggested to be around Cs_{40}. We find two linear intervals for the evolution of the cohesive energy of the clusters and obtain a bulk cohesive energy from extrapolation that agrees nicely with observed and calculated bulk cohesive energies.

ACKNOWLEDGMENTS

We thank the Royal Society of New Zealand for financial support through a Marsden grant and Philipp Mörschel (Marburg) for helpful discussions. This work was supported by the Royal Society of New Zealand (Marsden Grant No. MAU-313).

*p.a.schwerdtfeger@massey.ac.nz

[1] W. D. Knight, K. Clemenger, W. A. de Heer, W. A. Saunders, M. Y. Chou, and M. L. Cohen, Phys. Rev. Lett. **52**, 2141 (1984).
[2] W. A. de Heer, Rev. Mod. Phys. **65**, 611 (1993).
[3] W. D. Knight, K. Clemenger, W. A. de Heer, and W. A. Saunders, Phys. Rev. B **31**, 2539 (1985).
[4] D. E. Beck, Phys. Rev. B **30**, 6935 (1984).
[5] W. Ekardt, Phys. Rev. Lett. **52**, 1925 (1984).
[6] G. Tikhonov, V. Kasperovich, K. Wong, and V. V. Kresin, Phys. Rev. A **64**, 063202 (2001).
[7] I. S. Lim, M. Pernpointner, M. Seth, J. K. Laerdahl, and P. Schwerdtfeger, Phys. Rev. A **60**, 2822 (1999).
[8] I. S. Lim, P. Schwerdtfeger, T. Söhnel, and H. Stoll, J. Chem. Phys. **122**, 134307 (2005).

[9] P. Schwerdtfeger, M. Dolg, W. H. E. Schwarz, G. A. Bowmaker, and P. D. W. Boyd, J. Chem. Phys. **91**, 1762 (1989).
[10] P. Schwerdtfeger and G. A. Bowmaker, J. Chem. Phys. **100**, 4487 (1994).
[11] J. M. Amini and H. Gould, Phys. Rev. Lett. **91**, 153001 (2003).
[12] K. R. S. Chandrakumar, T. K. Ghanty, and S. K. Ghosh, Int. J. Quantum Chem. **105**, 166 (2005).
[13] P. Calaminici, A. M. Köster, and A. Vela, J. Chem. Phys. **113**, 2199 (2000).
[14] R. Antoine, D. Rayane, A. R. Allouche, M. Aubert-Frécon, E. Benichou, F. W. Dalby, Ph. Dugourd, and M. Broyer, J. Chem. Phys. **110**, 5568 (1999).
[15] D. Rayane, A. R. Allouche, E. Benichou, R. Antoine, M. Aubert-Frécon, Ph. Dugourd, M. Broyer, C. Ristori, F. Chandezon, B. A. Huber, and C. Guet, Eur. Phys. J. D **9**, 243 (1999).
[16] E. Benichou, R. Antoine, D. Rayane, B. Vezin, F. W. Dalby, Ph. Dugourd, M. Broyer, C. Ristori, F. Chandezon, B. A. Huber, J. C. Rocco, S. A. Blundell, and C. Guet, Phys. Rev. A **59**, R1 (1999).
[17] D. Plavšić, J. Koutecký, G. Pacchioni, and V. Bonačić-Koutecký, J. Phys. Chem. **87**, 1096 (1983).
[18] I. Boustani, W. Pewestorf, P. Fantucci, V. Bonačić-Koutecký, and J. Koutecký, Phys. Rev. B **35**, 9437 (1987).
[19] F. Wang, N. Andriopoulos, N. Wright, and E. I. von Nagy-Felsobuki, J. Cluster Sci. **2**, 203 (1991).
[20] M. Y. Chou, A. Cleland, and M. L. Cohen, Solid State Commun. **52**, 645 (1984).
[21] C. Bréchignac, Ph. Cahuzac, F. Carlier, M. de Frutos, and J. Ph. Roux, Phys. Rev. B **47**, 2271 (1993).
[22] G. Gardet, F. Rogemond, and H. Chermette, J. Chem. Phys. **105**, 9933 (1996).
[23] R. O. Jones, A. I. Lichtenstein, and J. Hutter, J. Chem. Phys. **106**, 4566 (1997).
[24] S. E. Wheeler and K. W. Sattelmeyer, P. v. R. Schleyer, and H. F. Schaefer III, J. Chem. Phys. **120**, 4683 (2004).
[25] S. A. Blundell, C. Guet, and R. R. Zope, Phys. Rev. Lett. **84**, 4826 (2000).
[26] C. R. Ekstrom, J. Schmiedmayer, M. S. Chapman, T. D. Hammond, and D. E. Pritchard, Phys. Rev. A **51**, 3883 (1995).
[27] P. Calaminici, K. Jug, and A. M. Köster, J. Chem. Phys. **111**, 4613 (1999).
[28] J. Guan, M. E. Casida, A. M. Köster, and D. R. Salahub, Phys. Rev. B **52**, 2184 (1995).
[29] I. Moullet, J. L. Martins, F. Reuse, and J. Buttet, Phys. Rev. B **42**, 11598 (1990).
[30] I. Moullet, J. L. Martins, F. Reuse, and J. Buttet, Phys. Rev. Lett. **65**, 476 (1990).
[31] K. B. Sophy, P. Calaminici, and S. Pal, J. Chem. Theory Comput. **3**, 716 (2007).
[32] G. Durand, F. Spiegelman, and A. R. Allouche, Eur. Phys. J. D **24**, 19 (2003).
[33] I. A. Solov'yov, A. V. Solov'yov, and W. Greiner, Phys. Rev. A **65**, 053203 (2002).
[34] L. Kronik, I. Vasiliev, and J. R. Chelikowsky, Phys. Rev. B **62**, 9992 (2000).
[35] S. Kümmel, T. Berkus, P.-G. Reinhard, and M. Brack, Eur. Phys. J. D **11**, 239 (2000).
[36] C. Bréchignac and Ph. Cahuzac, Chem. Phys. Lett. **117**, 365 (1985).
[37] A. vom Felde, J. Fink, and W. Ekardt, Phys. Rev. Lett. **61**, 2249 (1988).
[38] C. Bréchignac, Ph. Cahuzac, and J. Ph. Roux, J. Chem. Phys. **87**, 229 (1987).
[39] A. K. Ray and S. D. Altekar, Phys. Rev. B **42**, 1444 (1990).
[40] S. Mochizuki, K.-I. Inozume, and R. Ruppin, J. Phys.: Condens. Matter **11**, 6605 (1999).
[41] N. D. Bhaskar, R. P. Frueholz, C. M. Klimcak, and R. A. Cook, Phys. Rev. B **36**, 4418 (1987).
[42] N. D. Bhaskar and C. M. Klimcak, Int. J. Mass Spectrom. Ion Process. **113**, 13 (1992).
[43] R. Bahadur and R. B. McClurg, J. Chem. Phys. **121**, 12499 (2004).
[44] A. Kornath, A. Zoermer, and R. Ludwig, Inorg. Chem. **38**, 4696 (1999).
[45] M. Krauss and W. J. Stevens, Chem. Phys. Lett. **164**, 514 (1989).
[46] W. D. Hall and J. C. Zorn, Phys. Rev. A **10**, 1141 (1974).
[47] R. W. Molof, H. L. Schwartz, T. M. Miller, and B. Bederson, Phys. Rev. A **10**, 1131 (1974).
[48] I. S. Lim, P. Schwerdtfeger, B. Metz, and H. Stoll, J. Chem. Phys. **122**, 104103 (2005).
[49] A. Derevianko, W. R. Johnson, M. S. Safronova, and J. F. Babb, Phys. Rev. Lett. **82**, 3589 (1999).
[50] L. R. Hunter, D. Krause, Jr., S. Murthy, and T. W. Sung, Phys. Rev. A **37**, 3283 (1988).
[51] C. E. Tanner and C. Wieman, Phys. Rev. A **38**, 162 (1988).
[52] H. L. Zhou and D. W. Norcross, Phys. Rev. A **40**, 5048 (1989).
[53] L. R. Hunter, D. Krause, Jr., K. E. Miller, D. J. Berkeland, and M. G. Boshier, Opt. Commun. **94**, 210 (1992).
[54] D. DiBerardino, C. E. Tanner, and A. Sieradzan, Phys. Rev. A **57**, 4204 (1998).
[55] M. S. Safronova and C. W. Clark, Phys. Rev. A **69**, 040501(R) (2004).
[56] G. Höning, M. Czajkowski, M. Stock, and W. Demtröder, J. Chem. Phys. **71**, 2138 (1979).
[57] P. Fayet, J. P. Wolf, and L. Wöste, Phys. Rev. B **33**, 6792 (1986).
[58] I. Moullet, W. Andreoni, and P. Giannozzi, J. Chem. Phys. **90**, 7306 (1989).
[59] W. E. Ernst, R. Huber, S. Jiang, R. Beuc, M. Movre, and G. Pichler, J. Chem. Phys. **124**, 024313 (2006).
[60] J. Slater, F. H. Read, S. E. Novick, and W. C. Lineberger, Phys. Rev. A **17**, 201 (1978).
[61] K. M. McHugh, J. G. Eaton, G. H. Lee, H. W. Sarkas, L. H. Kidder, J. T. Snodgrass, M. R. Manaa, and K. H. Bowen, J. Chem. Phys. **91**, 3792 (1989).
[62] H. Fallgren, K. M. Brown, and T. P. Martin, Z. Phys. D: At., Mol. Clusters **19**, 81 (1991).
[63] H. Fallgren and T. P. Martin, Chem. Phys. Lett. **168**, 233 (1990).
[64] H. G. Limberger and T. P. Martin, J. Chem. Phys. **90**, 2979 (1989).
[65] H. G. Limberger and T. P. Martin, Z. Phys. D: At., Mol. Clusters **12**, 439 (1989).
[66] E. Eliav, M. J. Vilkas, Y. Ishikawa, and U. Kaldor, Chem. Phys. **311**, 163 (2005).
[67] T. Andersen, H. K. Haugen, and H. Hotop, J. Phys. Chem. Ref. Data **28**, 1511 (1999).
[68] J. Gspann, Z. Phys. D: At., Mol. Clusters **20**, 421 (1991).
[69] T. Bergmann, H. Limberger, and T. P. Martin, Phys. Rev. Lett. **60**, 1767 (1988).
[70] U. Lammers, G. Borstel, A. Mañanes, and J. A. Alonso, Z. Phys.

D: At., Mol. Clusters **17**, 203 (1990).
[71] A. Maanes, J. A. Alonso, U. Lammers, and G. Borstel, Phys. Rev. B **44**, 7273 (1991).
[72] Y. Li, E. Blaisten-Barojas, and D. A. Papaconstantopoulos, Phys. Rev. B **57**, 15519 (1998).
[73] S. K. Lai, P. J. Hsu, K. L. Wu, W. K. Liu, and M. Iwamatsu, J. Chem. Phys. **117**, 10715 (2002).
[74] A. Hermann, R. P. Krawczyk, M. Lein, P. Schwerdtfeger, I. P. Hamilton, and J. J. P. Stewart, Phys. Rev. A **76**, 013202 (2007).
[75] M. Ali (Basu), D. K. Maity, D. Das, and T. Mukherjee, J. Chem. Phys. **124**, 024325 (2006).
[76] F. S. Ham, Phys. Rev. Lett. **58**, 725 (1987).
[77] B. Assadollahzadeh, P. R. Bunker, and P. Schwerdtfeger, Chem. Phys. Lett. **451**, 262 (2008).
[78] M. J. Frisch, G. W. Trucks, H. B. Schlegel, G. E. Scuseria, M. A. Robb, J. R. Cheeseman, J. A. Montgomery, Jr., T. Vreven, K. N. Kudin, J. C. Burant, J. M. Millam, S. S. Iyengar, J. Tomasi, V. Barone, B. Mennucci, M. Cossi, G. Scalmani, N. Rega, G. A. Petersson, H. Nakatsuji, M. Hada, M. Ehara, K. Toyota, R. Fukuda, J. Hasegawa, M. Ishida, T. Nakajima, Y. Honda, O. Kitao, H. Nakai, M. Klene, X. Li, J. E. Knox, H. P. Hratchian, J. B. Cross, C. Adamo, J. Jaramillo, R. Gomperts, R. E. Stratmann, O. Yazyev, A. J. Austin, R. Cammi, C. Pomelli, J. W. Ochterski, P. Y. Ayala, K. Morokuma, G. A. Voth, P. Salvador, J. J. Dannenberg, V. G. Zakrzewski, S. Dapprich, A. D. Daniels, M. C. Strain, O. Farkas, D. K. Malick, A. D. Rabuck, K. Raghavachari, J. B. Foresman, J. V. Ortiz, Q. Cui, A. G. Baboul, S. Clifford, J. Cioslowski, B. B. Stefanov, G. Liu, A. Liashenko, P. Piskorz, I. Komaromi, R. L. Martin, D. J. Fox, T. Keith, M. A. Al-Laham, C. Y. Peng, A. Nanayakkara, M. Challacombe, P. M. W. Gill, B. Johnson, W. Chen, M. W. Wong, C. Gonzalez, and J. A. Pople, GAUSSIAN 03, Revision C.02, Gaussian, Inc., Pittsburgh, PA, 2003.
[79] S. Schäfer, B. Assadollahzadeh, M. Mehring, P. Schwerdtfeger, and R. Schäfer, J. Phys. Chem. A **112**, 12312 (2008).
[80] A. D. Becke, Phys. Rev. A **38**, 3098 (1988).
[81] J. P. Perdew, Phys. Rev. B **33**, 8822 (1986).
[82] P. Schwerdtfeger, in *Computational Aspects of Electric Polarizability Calculations: Atoms, Molecules and Clusters*, edited by G. Maroulis (IOS, Amsterdam, 2006), pp. 1–32.
[83] P. E. Blöchl, Phys. Rev. B **50**, 17953 (1994).
[84] G. Kresse and J. Furthmüller, Comput. Mater. Sci. **6**, 15 (1996).
[85] G. Kresse and D. Joubert, Phys. Rev. B **59**, 1758 (1999).
[86] J. P. Perdew, J. A. Chevary, S. H. Vosko, K. A. Jackson, M. R. Pederson, D. J. Singh, and C. Fiolhais, Phys. Rev. B **46**, 6671 (1992).
[87] J. P. Perdew, K. Burke, and M. Ernzerhof, Phys. Rev. Lett. **77**, 3865 (1996).
[88] S. H. Vosko, L. Wilk, and M. Nusair, Can. J. Phys. **58**, 1200 (1980).
[89] F. D. Murnaghan, Proc. Natl. Acad. Sci. U.S.A. **50**, 697 (1944).
[90] J. Li, X. Li, H.-J. Zhai, and L.-S. Wang, Science **299**, 864 (2003).
[91] C. A. Swenson, Phys. Rev. **99**, 423 (1955).
[92] In the jellium picture, an ideal conductor with spherical shape exhibits a polarizability according to $\alpha_{\text{classical}}=R^3$, where the positive background formed by the ions is denoted by a uniformly charged sphere of radius R. Electron spillout ultimately enhances the effective radius of the particle, i.e., $\alpha_{\text{classical}}=(R+\delta)^3$.
[93] A. J. Dekker, *Solid State Physics* (Macmillan, London, 1958).
[94] *CRC Handbook of Chemistry and Physics*, edited by D. R. Linde (CRC, Boca Raton, 2002).
[95] G. E. Moyano, R. Wesendrup, T. Söhnel, and P. Schwerdtfeger, Phys. Rev. Lett. **89**, 103401 (2002).
[96] R. Busani, M. Folkers, and O. Cheshnovsky, Phys. Rev. Lett. **81**, 3836 (1998).
[97] J. Wang, M. Yang, G. Wang, and J. Zhao, Chem. Phys. Lett. **367**, 448 (2003).
[98] K. A. Gschneidner, Jr., Solid State Phys. **16**, 275 (1964).
[99] F. W. Averill, Phys. Rev. B **6**, 3637 (1972).
[100] S. Carlesi, A. Franchini, V. Bortolani, and S. Martinelli, Phys. Rev. B **59**, 11716 (1999).
[101] D. D. Pollack, *Physical Properties of Materials for Engineers* (CRC, Boca Raton, 1993).
[102] O. P. Gupta, J. Phys. Soc. Jpn. **53**, 2575 (1984).
[103] N. Nücker and U. Buchenau, Phys. Rev. B **31**, 5479 (1985).